A novel high birefringence equal diameter circular-hole photonic crystal fiber*

GUO Jun-qi (郭俊启)**, ZHONG Yi** (钟懿)**, LIU Yu** (刘宇)****, YANG Xiao-hui** (杨晓辉)**, XIAO Ming-lang** (肖明朗)**, and ZHOU Min** (周敏)

Chongqing Municipal Key Laboratory of Photoelectronic Information Sensing and Transmitting Technology, Chongqing University of Posts and Telecommunications, Chongqing 400065, China

(Received 17 June 2017; Revised 7 August 2017)

A novel equal diameter circular-hole photonic crystal fiber (PCF) with high birefringence is proposed and numerically analyzed by employing the finite-element method. The proposed PCF's birefringence is 10^{-3}, which can reach 2 orders higher than that of traditional high birefringence fiber, and this equal diameter circular-hole structure reduces the difficulty of the actual drawing process. The effect of different parameters on the birefringence of this PCF is investigated, and the application of the Sagnac interferometer based on fiber filling technology in temperature sensing is studied. The result shows that the high birefringence PCF can be used in both optical communication and optical sensing fields.

Document code: A **Article ID:** 1673-1905(2017)05-0349-5

DOI https://doi.org/10.1007/s11801-017-7118-2

High birefringence fiber has important applications in fiber sensing and optical communication fields. Conventional fiber birefringence is low, and it needs to introduce materials to obtain high birefringence. Photonic crystal fiber (PCF) is a two-dimensional optical fiber[1,2], where air holes are periodically introduced in the cladding of quartz substrate. Benefited from its flexible structure design, the PCFs have great potential development and broad application prospect[3-6]. The high birefringence PCFs made of pure quartz material can be designed with different structures to improve optical fiber performance, and have the incomparable superiority to traditional high birefringence fiber. The high birefringence PCF's structure is flexibly designed through the introducing air holes with different sizes in the cladding or changing the shapes of the fiber core and cladding air holes for getting higher birefringence and excellent properties.

In recent years, with the rapidly increasing requirements of fiber properties applied in optical information transmission with high precision and velocity[7,8], plenty of high birefringence PCFs have been designed. Habib et al[9] proposed a micro-structural core PCF, whose birefringence reached 2.11×10^{-2}. Although this method can achieve high birefringence, the shape of air hole is not unified, which makes the production difficult. Habib et al[10] designed a type of high birefringence PCF, and the birefringence could be high as 3.79×10^{-2}, but some materials need to be introduced. Cai et al[11] proposed a dodecagonal photonic quasi-crystal fiber with high birefringence, the birefringence reached 3.86×10^{-2}, but the arrangement of the air hole has no rule which increases difficulties of the production process. Generally, most PCFs are formed by various kinds of irregular circular air holes in the cross section. There are few reports about high birefringence PCFs using pure circular air-holes in fiber cladding.

In this paper, we propose a new kind of high birefringence PCF structure. Some equal diameter circular holes are introduced in the quasi-rectangular arrangement PCF fiber, the transverse and longitudinal air hole spacing values are adjusted, a new type of PCF hybrid distribution structure is formed, whose birefringence can reach the magnitude of 10^{-3}. By simulating and adjusting the parameters of proposed structure firstly, we analyze the effect of structural parameter of PCF on the mode birefringence by full-vector finite-difference frequency-domain method, in order to find patterns obtained with the largest birefringence optical fiber structure parameters. Simulation results show that different structural parameters can make the birefringence increase at least two orders of magnitude than that of the traditional high birefringence fiber. PCF can achieve high birefringence

* This work has been supported by the National Natural Science Foundation of China (Nos.61301124, 61471075 and 61671091), the Basic Research Project of Chongqing Science and Technology Commission (Nos.cstc2014gjhz40001, cstc2015jcyjBX0068, cstc2014jcyjA1350, cstc2015jcyjB0360 and KJZH17115), the University Innovation Team Construction Plan of Smart Medical System and Core Technology, the Enhancement Plan of Chongqing Key Laboratory of Photoelectronic Information Sensing and Transmitting Technology, the Scientific and Technological Research Program of Chongqing Municipal Education Commission (No.KJ1704091), and the Funds of Chongqing University of Posts and Telecommunications (No.A2016-72).

** E-mail: liuyu@cqupt.edu.cn

by changing its aperture and arrangement, making it more suitable for practical application[12]. Finally, part of the air holes in this proposed PCF are selectively filled, and the temperature sensitivity based on the Sagnac interferometer is analyzed. It is shown that the PCF with high birefringence and easy drawing process can be applied in temperature sensing fields after filling functional materials.

We adjust the air hole structure of PCF and form a kind of the pure circular-hole PCF with high birefringence. The cross section structure of the PCF is shown in Fig.1. The air holes are arranged in a quasi-rectangular area near the fiber core, and the sizes of holes are all the same. The structural parameters are as follows: the air hole pitches are Λ=2.232 μm, Λ_x=2.86 μm and Λ_y=1.876 μm, the diameter of each circular air hole is d, the refractive index of the air hole is set as n=1, and the refractive index of the background silica is set as n=1.444.

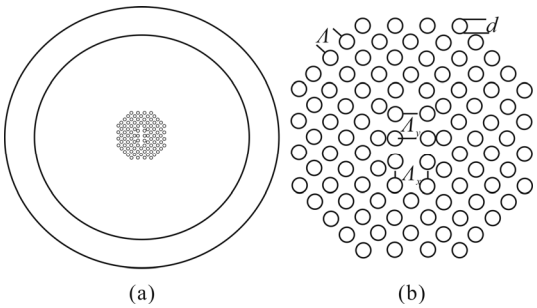

Fig.1 (a) Cross section of the pure circular-hole PCF; (b) The circular-hole arrangement in the fiber cladding

Birefringence index, as an important parameter for describing high birefringence PCF, is defined as the difference between the effective refractive indices of the x-polarization mode and the y-polarization mode[13,14]. The birefringence of the fundamental mode can be expressed as

$$B=\left|\mathrm{Re}\left(n_{\mathrm{eff}}^{y}-n_{\mathrm{eff}}^{x}\right)\right|, \tag{1}$$

where n_{eff}^{x} and n_{eff}^{y} are the effective refractive indices of the fundamental modes on x-polarization and y-polarization, respectively, and Re denotes real part.

Not only COMSOL software has high precision and accuracy, but also interface and operation are simple. The effective refractive indices of the fundamental modes can be calculated by COMSOL. The relationships between the effective refractive indices and wavelength of the fundamental modes are shown in Fig.2.

It can be seen from Fig.2 that in the short wavelength region, the effective refractive indices of the fundamental modes on x-polarization state and y-polarization state in PCF are almost the same, so there is no birefringence. With the increase of the wavelength, the birefringence increases obviously. The reason is that with the increase of wavelength, the mode field gradually penetrates into the cladding, and the penetration velocity of x-polarization mode is faster than that of y-polarization mode, which leads to the effective refractive index difference between the two polarization modes.

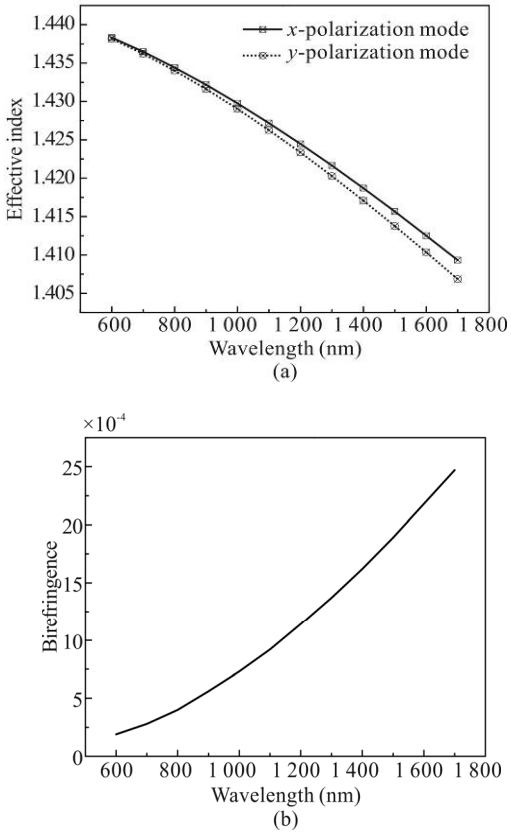

Fig.2 (a) The curves of fundamental mode field dispersion characteristics; (b) The curve of birefringence with wavelength

Fig.3 shows the mode field distributions of x-polarization state and y-polarization state at 1 550 nm. For the asymmetry of the core, the effective refractive indices of x-polarization mode and y-polarization mode are different. The effective refractive index of x-polarization mode is n_{eff}^{x}=1.414, and the effective refractive index of y-polarization mode is n_{eff}^{y}=1.412. Therefore, the fundamental mode birefringence at 1 550 nm is $B_1=|(n_{\mathrm{eff}}^{y}-n_{\mathrm{eff}}^{x})|=2.03\times10^{-3}$.

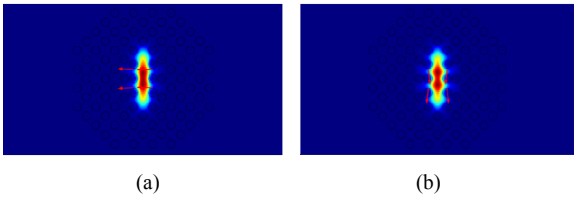

Fig.3 Distributions of (a) *x*-polarization and (b) *y*-polarization fundamental mode electrical fields at 1 550 nm

We study the polarization dependent loss at 1 330 nm and 1 550 nm. The ratio between constraint losses of *x*-polarization mode and *y*-polarization mode at λ=1 330 nm is 3.8:1 and the ratio at λ=1 550 nm is 1.76:1. So these two models can be transmitted at the same time.

In order to study the effect of different parameters on birefringence, we analyze the relationship of the air hole parameters and the birefringence, and Fig.4 shows birefringence of PCFs with different hole spacing of Λ_1=2.032 μm, Λ_2=2.132 μm, Λ_3=2.232 μm, Λ_4=2.332 μm and Λ_5=2.432 μm, respectively, where the air hole diameter is d=0.7 μm under the same wavelength of 1 550 nm.

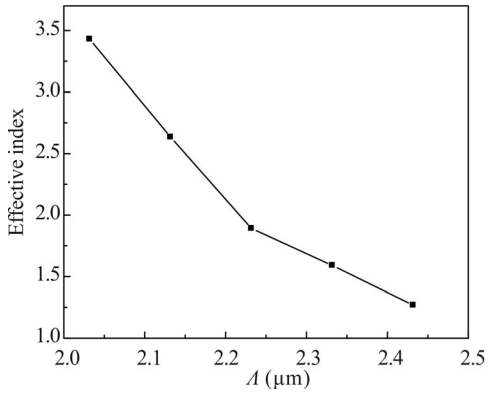

Fig.4 Curve of birefringence variation with different hole spacing Λ

Fig.4 shows that with the increase of Λ, the birefringence decreases gradually, which is due to the elliptical core PCF changing the core geometry to obtain high birefringence. The birefringence value of the model with Λ_1=2.032 μm is 3.42×10^{-3}, which is 1—2 orders of magnitude larger than that of the ordinary elliptical core. Although the birefringence of PCF with Λ_1=2.032 μm is the largest, there are some overlaps among the air holes in the PCFs with Λ_1=2.032 μm and Λ_2=2.132 μm as shown in Fig.5. Therefore, Λ_3=2.232 μm is the most appropriate.

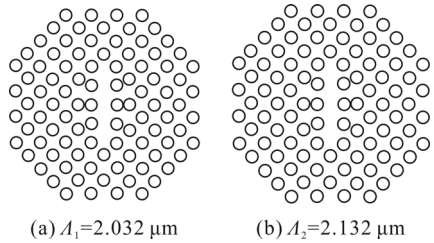

Fig.5 Cross sections of the PCFs with different hole spacing Λ_1 and Λ_2

Then, we change the elliptical core geometry to obtain high birefringence. Fig.6 shows PCF birefringence curve along with different air hole diameters of d=0.4 μm, 0.5 μm, 0.6 μm and 0.7 μm and the same hole spacing of Λ=2.232 μm at λ=1 550 nm.

Keeping the air hole spacing Λ=2.232 μm constant, with the increase of the air hole diameter d, the birefringence increases. At d=0.7 μm, the corresponding maximum birefringence value is 1.894×10^{-3}. If reduce the air hole spacing and increase the air hole diameter blindly to get a larger refractive index, it will make the air holes overlap. In this paper, we select moderate air hole pitch of Λ=2.232 μm, air hole diameter d=0.7 μm, and the maximum birefringence value at 1 550 nm is 3.42×10^{-3}.

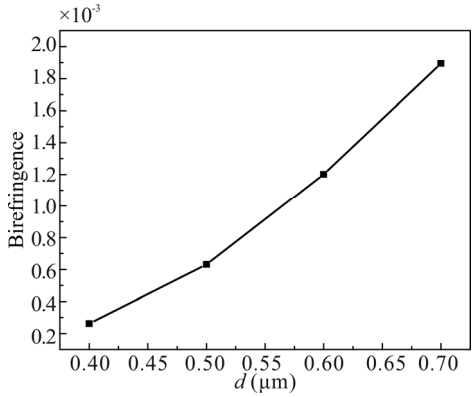

Fig.6 Curve of birefringence variation with different air hole diameters *d*

The structure has the potential to expand by adjusting the horizontal and vertical spacing, keeping d and Λ unchanged at the same wavelength of 1 550 nm. The curves of birefringence with different horizontal and vertical hole spacing values are shown in Fig.7.

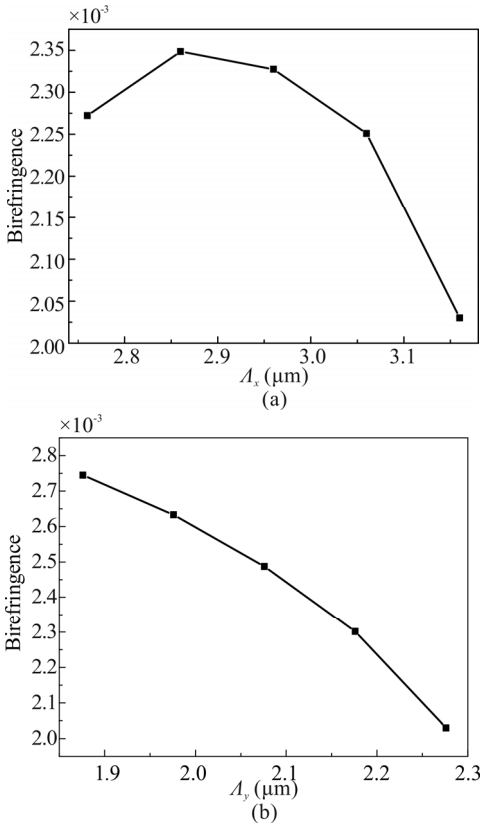

Fig.7 Curves of birefringence variation with different (a) horizontal and (b) vertical hole spacing

It can be seen from Fig.7(a) that with the increase of Λ_x, the birefringence increases at the beginning and then decreases. The core area becomes larger until reaches the maximum effective area, and the energy bounded in the core can't be effectively diffused into the cladding, so the birefringence reduces. It can be seen from Fig.7(b) that with the decrease of Λ_y, the basal area reduces, and the energy of the core can be effectively diffused into the cladding layer. According to the above analysis, we choose Λ_x=2.860 μm and Λ_y=1.876 μm to get a higher birefringence.

Through the above analyses, we can know that with the parameters as the air hole diameter d=0.7 μm, hole spacing Λ=2.232 μm, Λ_x=2.860 μm, Λ_y=1.876 μm and wavelength λ=1 550 nm, the birefringence is the highest as $B=3.42\times10^{-3}$. The cross section model proposed in this paper not only makes the process simple, but also has the potentiality by changing the distance among the three directions to meet the needs of the birefringence.

In the actual drawing process, the air holes are easily deformed into micro-elliptical air holes. Calculated with the other parameters remaining unchanged and changing the air hole to elliptical hole with a:b=1:1.01, the calculated birefringence B' is different from the original B about 0.01%. Therefore, the birefringence error produced by ellipticity in the actual drawing is within the acceptable range.

High birefringence PCF has important applications in Sagnac interferometer. For the Sagnac interferometer, two light beams divided by 3 dB coupler respectively go through the birefringent fiber clockwise and counter-clockwise to cause phase difference[15,16], which results in interference fringes. The local holes with selective filling are shown in Fig.8.

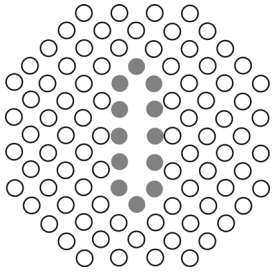

Fig.8 Cross section of the PCF selectively filled by liquid

The transmission interference spectrum formula is expressed as

$$Tr(\lambda)=\frac{1-\cos(\delta)}{2}, \tag{2}$$

where δ is the phase difference caused by the birefringent fiber with length of L and expressed as

$$\delta=2\pi LB(\lambda)/\lambda. \tag{3}$$

The thermo-optical coefficient of the filled liquid is $-0.000\,404\ °C^{-1}$ (ignoring the thermal coefficient of a pure silica substrate of $\sim 8.6\times10^{-6}\ K^{-1}$), the birefringence values of the PCF at different temperatures are calculated by using the finite element method. According to Eq.(2), when the length L is set to be 5 cm, the transmission spectra at different temperatures are shown in Fig.9. It can be seen that when the temperature changes from 25 °C to 35 °C, the resonant dip A shows the blue shift.

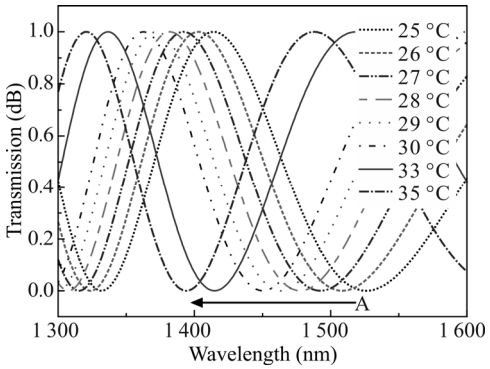

Fig.9 Transmission spectra of Sagnac interferometer with fiber length of 5 cm at different temperatures obtained by theoretical calculation

Fig.10 shows the drift tendency of resonant dip A. as the temperature increases, the drift velocity is getting slower, and the sensitivity to temperature is getting lower. The sensitivity at T=25 °C is about S=17 nm/°C, and the sensitivity at T=33 °C is about S=10 nm/°C. With the change in the refractive index of the air hole, the drift degree of resonance dip of Sagnac interferometer can be obtained to estimate the temperature change. It is shown that the PCF's structure proposed in this paper can be applied in temperature sensing fields after filling functional materials.

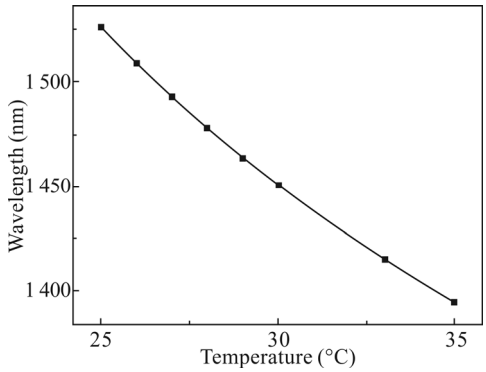

Fig.10 The tendency of the interference dip wavelength with temperature

In this paper, we design a kind of novel equal diameter circular-hole PCF, and investigate the effect of the air hole diameters, the hole spacing and the refractive index of material in hole on birefringence performance. The results indicate that the high birefringence can reach the order of 10^{-3}. Moreover, the structure has high birefringence and uniform shape and size of the air holes, which brings convenience to the production process. The new

PCF can be widely used in PCF laser, optical communication systems, polarization maintaining fibers and so on.

References

[1] Ortigosablanch A, Knight J C, Wadsworth W J, Arriaga J, Mangan B J, Birks T A and Russell P S, Optics Letters **25**, 1325 (2000).

[2] F. C. Favero, M. Becker, R. Spittel, M. Rothhardt, J. Kobelke and H. Bartelt, Photonic Sensors **3**, 208 (2013).

[3] Zhao Z, Acta Optica Sinica 31, 0900109 (2011). (in Chinese)

[4] Sun A, Wu Z and Huang H, Optics Communications **311**, 140 (2013).

[5] Kai Chen, Chenge Wang, Jinfang Wang and Xiaowu Shu, Journal of Optoelectronics·Laser **26**, 1406 (2015). (in Chinese)

[6] Guangwei Fu, Yang Liu, Xinghu Fu, Wenyu Yao, Xueqiang Liu and Weihong Bi, Journal of Optoelectronics·Laser **26**, 1639 (2015). (in Chinese)

[7] Y Chen, Q Han, W Yan, Y Yao and T Liu, IEEE Photonics Technology Letters **28**, 2665 (2016).

[8] Lin H Y, Chang H C, Journal of Lightwave Technology **10**, 1188 (1992).

[9] MS Habib, R Ahmad, MS Habib and SMA Razzak, Optik **125**, 4313 (2014).

[10] MS Habib, MS Habib, MI Hasan and SMA Razzak, Optical Fiber Technology **20**, 328 (2014).

[11] Cai W, Liu E, Feng B, Xiao W, Liu H, Wang Z, Wang S, Liang T and Liu J, Journal of the Optical Society of America A: Optics Image Science & Vision **33**, 2108 (2016).

[12] P Kumar, S K Pathak, A K Meher and S Mohapatra, A Unique Design of PCF with Zero Dispersion and High Birefringence, IEEE International Conference on Electronics and Communication Systems, 123 (2015).

[13] Jiang G, Fu Y and Huang Y, Optical Fiber Technology **26**, 163 (2015).

[14] Y Yue, G Kai, Z Wang, C Zhang, Y Lu, Y Li, T Sun, L Jin, J Liu, Y Liu, S Yuan and X Dong, IEEE Photonics Technology Letters **18**, 2032 (2006).

[15] M Chen, SG Yang, FF Yin, HW Chen and SZ Xie, Optoelectronics Letters **4**, 19 (2008).

[16] S Lu, W Li, H Guo and M Lu, Applied Optics **50**, 5798 (2011).